analytical chemistry

Article

pubs.acs.org/ac

# Microchamber Western Blotting Using Poly-L-Lysine Conjugated Polyacrylamide Gel for Blotting of Sodium Dodecyl Sulfate Coated Proteins

Minsub Chung,[†] Dohyun Kim,[†,‡,§] and Amy E. Herr*[,†]

[†]Department of Bioengineering, University of California, Berkeley, California 94720, United States

[‡]Department of Mechanical Engineering, Myongji University, Yongin, Gyeonggi-do 449-728, South Korea

Supporting Information

**ABSTRACT:** We report a novel strategy to immobilize sodium dodecyl sulfate (SDS)-coated proteins for fully integrated microfluidic Western blotting. Polyacrylamide gel copolymerized with a cationic polymer, poly-L-lysine, effectively immobilizes all sized proteins after sodium dodecyl sulfate polyacrylamide gel electrophoresis (SDS-PAGE), and enables SDS-PAGE and subsequent immuno-probing in an automated microfluidic chip. Design of a poly-L-lysine conjugated polyacrylamide gel allows optimization of SDS-protein immobilization strength in the blotting gel region of the microchamber. The dependence of protein capture behavior on both the concentration of copolymerized charges and poly-lysine length is studied and gives important insight into an electrostatic immobilization mechanism. Based on analysis of protein conformation, the immobilized proteins bind with partner antibody after SDS dilution. We demonstrate each step of the microchamber Western blot, including injection, separation, transfer, immobilization, blocking, and immunoblot. The approach advances microfluidic protein immunoblotting, which is directly relevant to the widely-used SDS-PAGE based slab-gel Western blot, while saving sample volume, labor, and assay time.

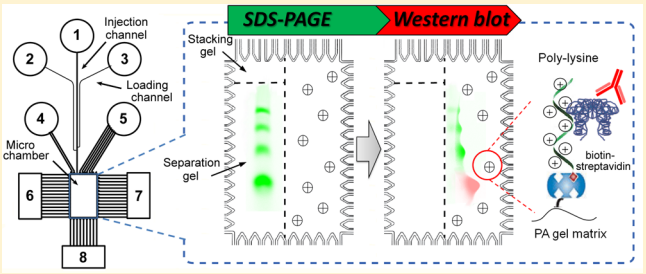


Western blotting is an indispensable analytical technique used to detect target proteins in biological samples separated by gel electrophoresis.[1,2] SDS-PAGE is by far the most common type of gel electrophoresis which employs polyacrylamide (PA) gels as a sieving matrix and SDS protein treatment to achieve uniform charge-to-mass ratio. The proteins, which are sized by the length of denatured polypeptides, are transferred to a fixation substrate, a so-called "blotting membrane" such as polyvinylidene fluoride (PVDF) or nitrocellulose (NC).[3] Antibody based probing of target proteins immobilized on the blotting membrane is performed after a series of blocking, washing, and developing processes and gives specific analytical information by correlating known antibody signal and molecular mass of the target antigen. The throughput and performance of SDS-PAGE and Western blot has been gradually improved by standardizing and commercializing the apparatus, reagents, and blotting membranes since the Western blot was introduced in 1979.[2] However, limited effort has been made to tackle the fundamental limitations that hinder progress until recently.

The major shortcoming of the conventional slab-gel Western blot is a resource-intensive and low-throughput nature. Slab-gel electrophoresis for protein sizing, the first step, takes 1−2 h for full separation and staining/destaining. The electroblotting step to transfer the sized proteins from PA gel to PVDF membrane is at least a 3-h process, and requires substantial preparation and manual intervention to assemble/disassemble the transfer stack and apparatus. The final antibody (Ab) probing step requires at least 4 h for a series of laborious handling steps including blocking, Ab binding, washing, and developing. Moreover, the consumption of sample, reagents, and expensive antibody (∼10 μg) is copious. Continued innovation is needed to overcome these deficiencies while maintaining the analytical power and universal validity of Western blotting.[4]

Microanalytical systems have made notable improvements to overcome limitations of conventional slab-gel Western blotting. Our laboratory pioneered a semiautomated microfluidic device for native Western blotting.[4] This immobilized antibody-based design integrates fast and programmable on-chip electrophoresis, electrotransfer, and immunoassay with ultralow sample consumption in a single chip. However, microfluidic integration of SDS-PAGE and antibody probing presents challenges. One major challenge is immobilization of all sized proteins in a manner suitable for subsequent antibody probing. Dilution or removal of SDS from the SDS-protein complexes is needed owing to reduced affinity between detergent-coated proteins and antibodies in the presence of SDS. These obstacles have been addressed by various approaches. For the integration of SDS-PAGE to the microfluidic system, a high-density

**Received:** April 6, 2013
**Accepted:** July 14, 2013
**Published:** July 15, 2013

  

polyacrylamide membrane "filter", through which only small SDS molecules can pass, was used to remove SDS from sized proteins.[5] The stripping of SDS due to the mobility difference between SDS and proteins during electrotransfer successfully prevented deleterious effects of SDS.[6] Though multianalyte blotting[7] can immobilize selected native protein targets on strips of serial blotting gels, electrostatic immobilization on charge-functionalized PA gel enabled pan-analyte (nonspecific) capture of all sized proteins complexed with the cationic detergent CTAB (cetyl trimethylammonium bromide),[8] followed by subsequent immunoassay with electrophoretically introduced antibody. Although this system showed size-based separation and immunoblotting, SDS-PAGE is a more relevant molecular assay widely used by the research community. Recently, a light-activated protein capture approach[9] was used to immobilize all sized SDS-coated proteins covalently thus enabling microfluidic Western blotting in a single microchannel.[10] However, since this immobilization mechanism varies substantially from the traditional Western blot, not all of the accumulated data and know-how of Western blotting can be applied directly.

Despite breakthroughs, the detailed mechanisms of protein blotting, SDS removal, and protein renaturation are elusive. In a conventional Western blot, the mechanism of protein binding is complex and thought to be related to hydrophobic interaction and dipole moment on the polymer membrane (NC or PVDF).[11] SDS removal occurs during transfer by dilution or electrophoretically, but the protein structure after blotting and the SDS removal is not known.[12] The kinetics of protein immobilization in the microfluidic system have been investigated for antibody-based blotting[7] and covalent immobilization.[9] Nonetheless, the interrogation of SDS removal and protein renaturation has been only possible for green fluorescent protein[5] or by indirect methods.[6] Methods for study of interactions between SDS and proteins (including reversible binding of fluorescent dyes,[13,14] tryptophan quenching,[15] and circular dichroism, [13] are difficult to apply to protein blotting in a microfluidic chip. Though protein renaturation was not necessary when a nondenaturing detergent, CTAB, was used,[8] detergent removal was still required because CTAB can disturb antibody binding.

In this study, we integrate SDS-PAGE and Western blotting into a single microfluidic platform. By employing electrostatic immobilization,[8] sized, negatively-charged SDS-coated proteins are immobilized on a positive charge-functionalized PA gel. The adjustable and well-defined cationic polymer, poly-L-lysine (PL, Figure 1 and Figure S1 in the Supporting Information), enables efficient immobilization of all sized proteins by SDS-PAGE and enables performance advances to expand the applicability of microfluidic protein analysis. As we can manipulate this capture agent, the immobilization strength and pattern can be adjusted to achieve optimal conditions for the desired application. By modification of PL, the nature of protein immobilization can be elucidated through a detailed study of capture behavior. Moreover, by applying self-quenching of protein-conjugated dyes for the first time in a microfluidic Western, SDS removal and protein renaturation[16] is monitored during the immobilization process. Lastly, antibody probing is performed in the same buffer and blocking agent as a conventional Western blot. Hence, the accumulated experience and knowledge of conventional Western blotting can be directly applied to this microanalytical system. Our new microfluidic approach and thorough characterization forges a clear path toward rapid, automated, low-sample consuming protein research relevant to life science and clinical research.

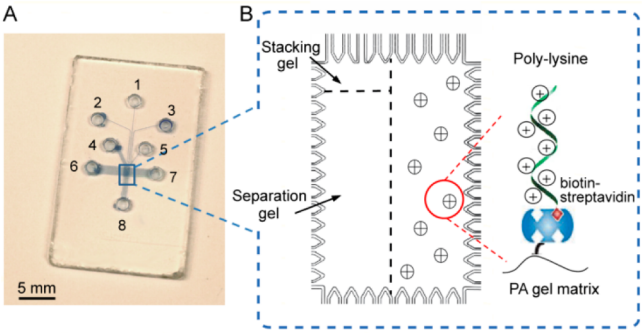


**Figure 1.** (A) Photograph of glass microfluidic device with microchannels and numbered reservoir holes. (B) Schematic design of the patterned microchamber for microfluidic Western blotting. A central microchamber is surrounded by microchannels for sample/reagent introduction and transport using electric field control. The microchamber houses spatially photopatterned functional PA gels: stacking gel (large pore) for protein loading and stacking, separation gel (small pore) for SDS-PAGE, and PL-PA blotting gel for protein immobilization and immunoblotting. Positively charged PL is copolymerized to a PA gel by biotin-streptavidin linker (not to scale).

## EXPERIMENTAL PROCEDURES

**Reagents.** C-reactive protein (CRP, 25 kDa) was from R&D systems (Minneapolis, MN). Ovalbumin (OVA, 45 kDa) and bovine serum albumin (BSA, 68 kDa) were from Invitrogen (Carlsbad, CA). Phosphorylase b (Phos, 97.2 kDa) and carbonic anhydrase (CA, 29 kDa) were from Abcam (Cambridge, MA). All the proteins were purchased with fluorophore conjugation except CRP which was conjugated in-house with Alexa Fluor 488 (AF488, Invitrogen) following the manufacturer's instructions. Rabbit polyclonal anti-CRP (Abcam) and mouse monoclonal anti-SOD-2 (Santa Cruz Biotechnology) were conjugated in-house with Atto 550 (Sigma). The proteins and antibodies were all solubilized in Tris-glycine (TG) buffer. The proteins to be analyzed are denatured and reduced in 2% SDS (Sigma) and 0.1 M dithiothreitol (DTT) solution.

Various molecular weights of poly-L-lysine were purchased from Sigma. Throughout this report, they are classified by average molecular weight PL25 (18−32 kDa), PL50 (30−70 kDa), PL100 (70−130 kDa), and PL150 (100−200 kDa).

**Biotinylation Protocol and Degree of Labeling of PL.** We utilized a streptavidin−biotin linkage chemistry to incorporate PL into the PA blotting gel. The PL was conjugated with biotin by following the manufacturer's instructions of the Chromalink biotin labeling kit (Solulink, San Diego, CA) with minor modification. This kit provides a sulfo-NHS-biotin conjugated with UV-traceable linker which enables spectroscopic quantification of biotin. The chemical structure and conjugation reaction are shown in Figure S1 in the Supporting Information. At room temperature, a three-molar-excess amount of NHS-biotin was added to 5 mg each of PL (5 mg in 1 mL of 0.1 M PBS buffer) and incubated for 90 min. The mixture was then dialyzed against deionized water to remove unconjugated biotin. The absorbance value at 354 nm ($\varepsilon$ = 29 000) was measured to determine the amount of conjugated biotin. The solution was then dried by Speedvac (Virtis Benchtop K series, Virtis, Gardiner, NY) to measure its dry


dx.doi.org/10.1021/ac401012j | Anal. Chem. 2013, 85, 7753−7761

weight. The degree of labeling (DOL, number of biotins per PL molecule) ranged from 1.5 to 2.3.

**Fabrication of Microchip for Microfluidic WB.** The fabrication processes for wet-etched glass microfluidic chips (Figure 1A) and photopatterning of PA gel regions in a glass microdevice are described in our previous studies[8] and in the Supporting Information. All PA gels used in this study were photopolymerized using acrylamide/bisacrylamide (Sigma, 3.3%C w/w cross-linker) with 0.2% w/v photoinitiator (VA-086, Wako Chemical, Richmond, VA). To fabricate PL-PA blotting gels (Figure 1B) for electrostatic protein immobilization, charged moieties, either PL or diallyldimethylammonium chloride (DADMAC, Sigma, p$K$ = 10.5), were included in the polymer precursor solution. Biotinylated poly lysine (PL) was copolymerized in the polyacylamide (PA) gels after overnight incubation with a 3.8 $\mu$M streptavidin acrylamide linker (Invitrogen) in 1× TG buffer. For comparison of charge capture efficiency, DADMAC was copolymerized into the PA gel without modification. Gel precursor solutions for the PL-PA blotting gel were prepared by diluting 30% T, 3.3% C (w/v) acrylamide/bis-acrylamide to achieve a 4.5% T total acrylamide concentration in 1× TG buffer with 0.2% (w/v) VA-086 photoinitiator, 3.8 $\mu$M of streptavidin acrylamide, and 0−3.2 $\mu$M of biotinylated PL. All PA gels were photopatterned under UV exposure in the following order: PL-PA blotting gel (4.5% T), separation gel (6% T), and stacking gel (3% T).

**Automated Microfluidic Assay Procedure.** Electrophoretic protein migration was controlled by applying a sequence of voltages and currents via eight access holes (Figure 1A) using a custom built, eight-channel high-voltage sequencer. A typical voltage/current program for the PL-PA blotting gel characterization (protein loading, separation, transfer) and WB assay (protein loading, separation, transfer, blocking, immunoblotting) is shown in Table S-1 in the Supporting Information. SDS was not added to the gel precursor solution prior to photopolymerization because SDS coats the PL and interferes with protein capture (this SDS blocking is used to assess steric effects of PL, detailed in the Supporting Information). SDS (0.1% in 1× TG) was loaded to access holes no. 1, no. 2, and no. 3 and electrophoretically introduced into sample loading channels (from access hole no. 2 and no. 3) for 10 min. Then, SDS was electrophoretically injected as a narrow band to define the separation region for 10 min before protein sample loading. The denatured and reduced SDS-protein mixture was added from hole no. 3 to hole no. 1 to form an injection plug in the T junction. As described elsewhere,[4] the injected protein plug was stacked at the interface between the stacking gel and separation gel, and separated proteins were transferred to the PL-PA blotting gel for immobilization, followed by BSA blocking and Ab probing.

**Fluorescence Imaging and Image Analysis.** An epifluorescence microscope (IX-70, Olympus, Center Valley, PA) was used for data collection via a Peltier-cooled CCD camera (CoolSNAP HQ$^2$, 1392 × 1030 resolution, Photometrics, Tucson, AZ). Imaging was conducted using a 100 W mercury lamp (Olympus), 10× objective (UPlanFL, NA = 0.3, Olympus). XF100-3 and XF111-2 filter sets (Omega Optical, Brattleboro, VT) were used for green and red fluorescence, respectively. Images were captured under 100 ms exposure times and 1 × 1 pixel binning. ImageJ software (NIH) and Matlab (Mathworks) were used for image analysis including calculation of separation resolution and signal-to-noise ratio. Protein material was quantified using the integrated fluorescence intensity with background subtraction. The fluorescence intensity curve, a function of migration distance ($x$), was generated from a $y$-axis intensity average of the two-dimensional fluorescence image. Protein immobilization efficiency was calculated from material retention on the PL-PA blotting gel. Material retention was defined as the ratio (%) of the fluorescence signal from protein zones before (in the separation gel) and after immobilization (in the PL-PA blotting gel).

## RESULTS AND DISCUSSION

**Strategy for Immobilization of SDS−Protein Complexes.** Western blotting with pan-protein immobilization after sizing is the most widely used blotting assay.[2] To broaden applicability of the microchamber Western blotting assay, we sought to introduce integrated protein blotting conducive to nonspecific immobilization of all SDS-coated proteins after SDS-PAGE. In addition to broadening applicability, postsizing protein immobilization would obviate SDS dilution and/or SDS removal steps used prior to immobilization, significantly simplifying the microfluidic assay workflow and improving assay throughput. The blotting region must immobilize (blot) SDS-coated proteins and be compatible with the microchamber-based Western blotting assay. To create a blotting region conducive to immobilization of SDS-coated proteins, we investigated a PL conjugated PA gel blotting region. PL, a cationic polymer widely studied and employed for cell adhesion and drug encapsulation,[17−19] offers adjustable physicochemical properties (e.g., overall charge and macromolecular length), an attribute attractive for both study and optimization of protein immobilization in the blotting gel.

Briefly, the microchamber Western blot integrates all steps of a Western blotting assay, sizing, electrotransfer, blotting and probing, in one monolithic device (Figure 1).[4,8] To achieve this, the microchamber houses discrete photopatterned separation and blotting gels flanked by a supporting microchannel network (e.g., cross injector at chamber top, electric-field control channels along periphery). As detailed previously, a plug of protein sample is electrophoretically loaded at the injection junction (see the Experimental Procedures for details). Once the plug enters the microchamber, species stack at the large-to-small pore-size interface of a stacking (3% T) and separation (6% T) gel. Proteins are separated according to molecular mass, akin to conventional SDS-PAGE. Affording more function than simply that of a tiny sizing slab gel, the microchamber supports controlled electrotransfer of all sized proteins from the separation gel to the blotting gel. The rapid electrotransfer is initiated by a transverse electric field. To achieve effective blotting, for subsequent probing with antibodies, immobilization should yield minimal losses in both separation resolution (from the sizing separation axis) and sample material.

Here, we pursued PL incorporation in PA gels using a biotin-streptavidin linkage. During photopatterning of the blotting region, streptavidin-acrylamide linker was included in the PA gel precursor solution. To incorporate PL in the streptavidin containing PA gel, biotin was covalently attached to the $\varepsilon$-amino groups of PL (see Figure S1 in the Supporting Information).

**Protein Immobilization in the PL-PA Blotting Gel.** To investigate the capacity of a PL-conjugated PA blotting gel to immobilize sized proteins, we completed microchamber-based sizing of a three protein ladder: BSA (66 kDa), OVA (45 kDa),


dx.doi.org/10.1021/ac401012j | Anal. Chem. 2013, 85, 7753−7761

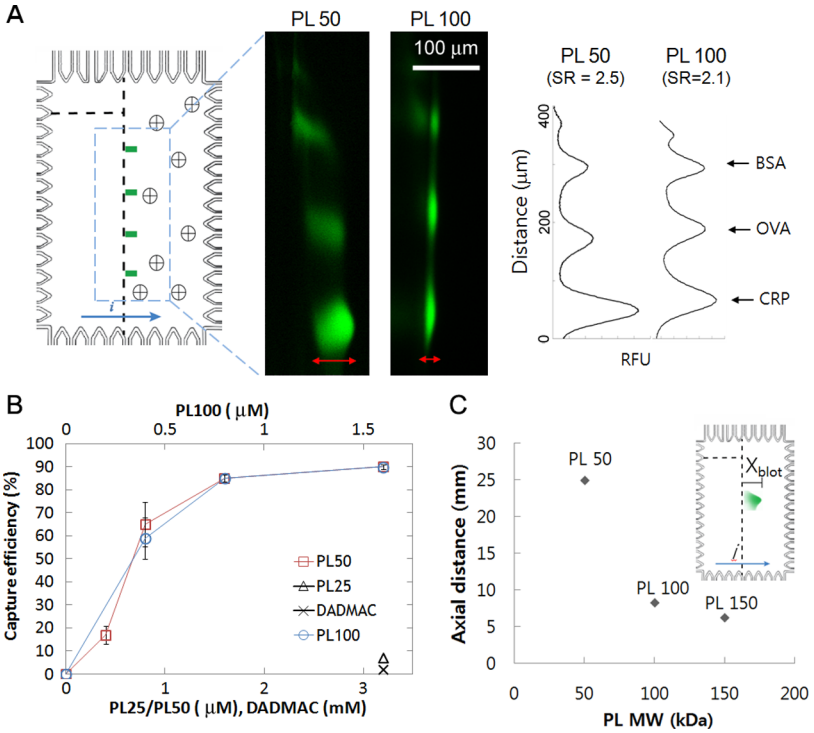


**Figure 2.** SDS–protein complex immobilization in a charged PA blotting gel. (A) Immobilization of a protein ladder (CRP, OVA, and BSA) with PL50 or PL100 in a PA blotting gel. The penetration distance of CRP is indicated by a red arrow. Fluorescence intensity profile shows similar sizing information after immobilization regardless of the band size. (B) Immobilization efficiency by varying charge density of PL-PA blotting gel containing DADMAC (×), PL25 (△), PL50 (□), or PL100 (○). The *x*-axes for concentration of PL50 and PL100 are scaled to match their charge density reflecting that PL100 has two times more charge density than the same amount of PL50. (C) The penetration distance of CRP plotted vs the molecular weight of PL. The inset illustrates how the distance is determined.

and CRP (25 kDa). A 4.5% T/3.3% C acrylamide/bis-acrylamide (29:1) PA gel was employed in the blotting region with various concentrations of PL50 and PL100 assessed (Figure 2). As compared to a larger molecular mass PL (PL100), the lower molecular mass PL (PL50) yields more dispersed capture. The immobilized protein distribution penetrates into the blotting gel (laterally), with an on average penetration to a ∼20 $\mu$m-wide region of PL50-PA blotting gel, while the PL100-immobilized protein distributions compressed near the interface of the PL-PA blotting gel (on average ∼8 $\mu$m wide zones). In both cases characterized here, the PL-PA blotting gel retains the sizing information and separation resolution (SR) after immobilization as observed from fluorescence micrographs, represented by average SR: from 2.7 to 2.5 after immobilization for PL50 and from 2.7 to 2.1 for PL100 (Figure 2A). The electrotransfer field strength was 45 V/cm in both cases.

For comparison, we also measured the immobilization efficiency on an alternative charge-grafted gel with cationic monomer, DADMAC (Sigma, p$K_a$ = 10.5). The DADMAC PA gel consisted of a positively charged monomer copolymerized with acrylamide that resulted in a hypothetically distributed charge instead of point charge.[8] We observed that, though 3 mM of DADMAC (equivalent charge density as 4.4 $\mu$M of PL100) was copolymerized to a PL-PA blotting gel, no measurable immobilization of SDS–protein complex was detected. Though the immobilization efficiency is slightly increased at an increased concentration of 10 mM, control of the electric field was difficult during protein transfer to the PL-PA blotting gel due to strong concentration polarization. This concentration polarization suggests the presence of a high-density of excess surface charge in the blotting gel.[8] For a given charge density, the PL-PA blotting gel enables stronger protein immobilization than the DADMAC copolymerized PA blotting gel. This result agrees with previous studies, where the negative point charges provided by $\beta$-gal showed much higher immobilization efficiency than negative distributed charge by Immobiline.[8] We hypothesize that while the highly charged PL protrudes into a pore, singly charged DADMAC molecules may be distributed in a dispersed manner around the PA network. The protruding PL may be more accessible to the SDS-protein electromigrating through the pores, thus the resultant force is potentially higher than in the DADMAC case.

We next sought to investigate the effect of PL length on protein immobilization in the PL-PA blotting gel. Various lengths of PL from 25, 50, 100, and 150 kDa (average MW, see the Experimental Procedures for the range of MW) while maintaining the overall charge density constant were incorporated in the PA blotting gel and subsequent protein immobilization was assessed. With all other conditions held constant, sized proteins were electro-transferred to and through PL-PA blotting gels with different charge characteristics. Figure 2B shows that immobilization efficiency for fluorescently labeled CA increases with increasing charge density up to 0.8 $\mu$M PL100 (same charge density as 1.6 $\mu$M PL50). We observe maximum protein immobilization with 0.8 $\mu$M PL100 and higher charge densities (e.g., 0.8 $\mu$M PL50). The correlation between the immobilization efficiency and the PL concentration suggests that PL is responsible for the immobilization of SDS–protein complexes. PL25 showed only trace amounts of protein immobilization (slightly more than DADMAC). As DADMAC and PL25 showed only trace protein immobiliza-


dx.doi.org/10.1021/ac401012j | *Anal. Chem.* 2013, 85, 7753–7761

tion, the accessibility of charged moieties is important. The charge distributed in the PA network is hypothesized as too diffuse in the PL25 case, so not particularly effective when many counterions are available for charge screening. We further hypothesize that the longer PL is more accessible (higher effective binding constant), as evidenced by the highly effective protein immobilization observed. The behavior of PL150 was indistinguishable from that of PL100 (Figure 2C).

To scrutinize the possibility that the presence of PL in the PA network obstructs migration of large SDS−protein complexes, we examined protein mobility in SDS-blocked PL-PA gels. By varying the size of PL conjugated to the PA gel and by subsequent neutralization of PL charge (via SDS blocking), we sought to investigate possible steric retardation of target protein migration through the PL-PA gels. After electrophoretically introducing a high concentration of SDS (0.2%) to the PL-PA gel, SDS-coated BSA and CRP were electrophoresed through the SDS-blocked PL-PA gel. Several gels housing PLs of different lengths were investigated (i.e., no PL, 1.6 $\mu$M PL50, or 0.8 $\mu$M PL100, matching the total amount of polymer). First, we observed trace immobilization (<1%) of proteins suggesting both that the SDS blocking of PL was effective at reducing electrostatic interactions and that protein immobilization via steric effects was minimal. Next, the mobility of the BSA and CRP were compared (Table S2 in the Supporting Information), allowing assessment of steric hindrance by the neutralized PL-conjugated PA gel. We observed comparable protein mobilities in PA gels with no PL and in PA gels with PL50. We observed lower protein mobility in PA gels conjugated with PL100. In each case, we observed similar mobility retardation for both BSA and CRP. These observations suggest that steric effects become significant with large polymer incorporation (i.e., PL100), probably by reducing effective pore size. The steric impedance of protein mobility by large PL may further suggest a higher probability for PL-protein binding in these gels, owing to both better accessibility of reaction partners and longer reaction times.

The impact of PL length can be represented by penetration distance of each resolved protein zone laterally into the blotting gel ($X_{blot}$) (Figure 2C). The length $X_{blot}$ is defined as the lateral penetration distance of a captured band (in the direction of transfer electric field) from the separation/blotting gel interface that contains 90% of total integrated intensity. We can understand the effect of PL length on the penetration distance by considering the interplay of two processes important to blotting in the microchamber: electromigration and reaction. Assuming the interaction between the migrating SDS−protein complex and PL in the PL-PA blotting gel follows a first order Langmuir binding model,[20] the binding reaction can be expressed as[7]

$$C + b_{PL} \underset{k_{off}}{\overset{k_{on}}{\rightleftarrows}} C_{bound}$$

where $C$ is the concentration of free protein, $C_{bound}$ is bound protein to PL, $b_{PL}$ is unoccupied binding sites, $k_{on}$ is association rate constant, and $k_{off}$ is dissociation rate constant. The available binding sites ($b_{PL}$) in this system may not be equally available to all proteins thus deviating from a typical Langmuir binding model. For example, the terminal end of PL may be more accessible to protein interaction, thus yielding an effective $b_{PL}$ for PL100 that could be higher than that for the same concentration of PL50. For this system, the nondimensional Damköhler number ($Da$) represents the ratio of reactive flux (determined by $k_{on}$ and availability of binding sites) to the mass transport flux (electromigration). Specifically, $Da = Lk_{on}b_{PL}/\mu_o E$ where $L$ is the width of the blotting region, $\mu_o$ represents the electrophoretic mobility of the analyte, and $E$ is the applied lateral electric field strength; thus $\mu_o E$ represents the analyte electromigration speed through the blotting region.[21,22] Hence, $Da$ describes the relationship between two time scales: electromigration time ($L/\mu_o E$) and binding reaction time ($1/k_{on}b_{PL}$). In this context, when the value of at high $Da$ (>10), the slowly migrating protein target in the PL-PA blotting gel allows enough time for binding reaction. Thus, the system is mass transport limited. When the value of $Da$ is low (<1), the protein migrates through the blotting gel too rapidly for binding and the system is reaction limited. Because the difference in $X_{blot}$ changed with $k_{on}Cb_{PL}$ (association rate) differences while the initial $C$, $\mu_o$, $E$, and $L$ were the same for each case, the characteristic of the reaction limited regime was observed in this immobilization system. That is, the variable considered here is more prominently changing the $k_{on}$ (effectively) and concentration of accessible binding sites than the electrotransport time scales (i.e., $E$ strength). As detailed in Table S2 in the Supporting Information, we observed a 5% mobility decrease in PL50-PA gels blocked with SDS and a 20% reduction in mobility in PL100-PA gels neutralized by SDS. We hypothesize that PL in the PA gel network may, in some instances, sterically impede protein electromigration. While steric interactions likely play a role in observed analyte mobilities, the conditions studied here suggest that steric hindrance alone may not be adequate to fully explain the $^1/_3$ shorter $X_{blot}$ length required for blotting on PL100-PA gels, as compared to the $X_{blot}$ length needed for blotting on PL50-PA gels. Consequently, we further hypothesize that physical accessibility of PL charge-binding sites to electromigrating proteins may also notably influence blotting (immobilization). The charge-to-charge attraction force between migrating SDS−protein complexes and less charged and less accessible PL50 will be weaker than that of PL100 or PL150, thus the excess proteins not yet captured by PL50 migrate further until they are all captured. Note that $X_{blot}$ of CRP is depicted in Figure 2C showing a fast-moving, less charged low MW protein that penetrates deeply. The dispersed bands by PL50 are more visible and free of the boundary effect, while the concentrated bands by PL100 give higher signal.

**Role of SDS in the PL-PA Immobilization Scheme.** We next sought to understand the role of SDS in protein immobilization after SDS-PAGE. We sought to monitor (1) the amount of protein immobilized on the PL-PA blotting gel and, simultaneously, (2) the dissociation of SDS from a PL-immobilized SDS−protein complex under an applied transverse electric field. We employed a model protein (CA) labeled with two fluorophores, Alexa Fluor 488 (DOL = 4.2) and Alexa Fluor 568 (DOL = 0.3), to minimize the population of CA protein with more than one AF568 (see schematics of Figure 3 inset and the Supporting Information for detail).

A high degree of labeling in the AF488 channel is hypothesized to give a qualitative indication of protein renaturation owing to use of the homo-FRET (Förster resonance energy transfer) or self-quenching phenomena (as is especially relevant to such multilabeled proteins[23,24]). When a highly labeled protein is denatured, the dye molecules should fluorescence maximally. With SDS removal and protein refolding, the homo-FRET phenomena should come into play, as the dye molecules pack more closely than in the


dx.doi.org/10.1021/ac401012j | Anal. Chem. 2013, 85, 7753−7761

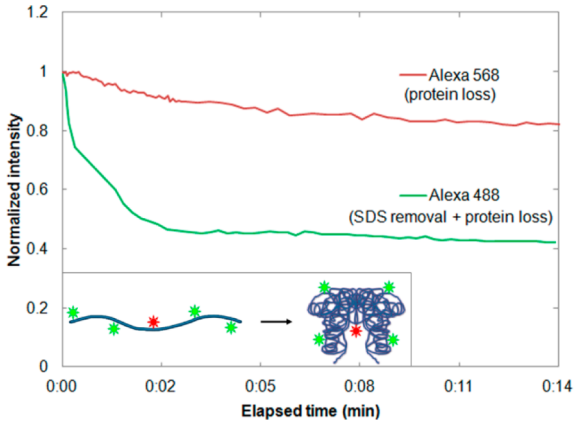


**Figure 3.** Protein loss and SDS removal are simultaneously monitored. The multilabeled AF488 fluorescence is SDS-dependent, while single-labeled AF568 fluorescence is SDS-independent. Fluorescence intensity profile scaled for the maximum intensity of each trace. The inset illustrates refolding of immobilized protein during SDS removal. Self-quenching between green dyes becomes important as their average distance decreases in renatured protein, while red dye is unaffected.

denatured protein case (Figure 3 inset). Thus, the refolded protein should exhibit lower fluorescence than the denatured protein, owing to self-quenching (Figure S2 in the Supporting Information). Via the same principle, a single-fluorophore labeled protein should exhibit negligible difference in fluorescence with or without SDS (~5%), as insufficient levels of dye molecules are present to self-quench.

To tease apart the levels of protein and SDS present, reduced and denatured dual-labeled CA was injected into the microchamber and captured on the PL-PA blotting gel (1.6 $\mu$M PL100) as before. The intensity of green (AF488) and red (AF568) fluorescence was monitored after protein immobilization while applying a transverse electric field ($E$ = 45 V/cm). Roughly 15% of the initially captured protein was electrophoretically washed away over the course of 15 min (Figure 3), as indicated in the red spectral channel (AF568, not SDS dependent). The time-course suggests a gradual loss of protein material from the PL-PA blotting gel. In contrast, the SDS-sensitive green fluorescence channel rapidly decreased by half in 2 min. The rapid decrease in green fluorescence signal is attributed to self-quenching during immobilized protein refolding stemming from SDS removal.

The resultant fluorescence profile during the electrophoretic wash provides important information about the binding mechanism after protein capture. The observed behavior suggests that (1) SDS does indeed dissociate from SDS–protein complexes after electrostatic immobilization, (2) even if the bound protein loses most of its charge by SDS removal, there are enough interactions between PL and the protein to maintain protein immobilization to a significant degree, and (3) the SDS-coated, denatured protein refolds to some degree after PL-mediated immobilization.

Taken together, we hypothesize that when SDS-coated proteins migrate through the PL-PA blotting gel, electrostatic attraction may be dominant initially. We observe that positively charged lactoferrin is less efficiently immobilized than SDS-coated, denatured lactoferrin. Although the Debye length in 1× TG buffer is a few nanometers,[25] the large size and high surface area of PL could become accessible. The size of individual molecules of PL can only be determined broadly because they are in a random coil structure[26] in the pH and buffer conditions used in this study. On the basis of the size of a random coiled homopolymer,[27] the length of PL50 and PL100 can be estimated as 12 and 22 nm, respectively. These polymers may adopt stretched conformations under an applied electric field,[28] as could be the case during protein immobilization. Because the apparent pore size of 4.5% T and 3.3% C PA gel is

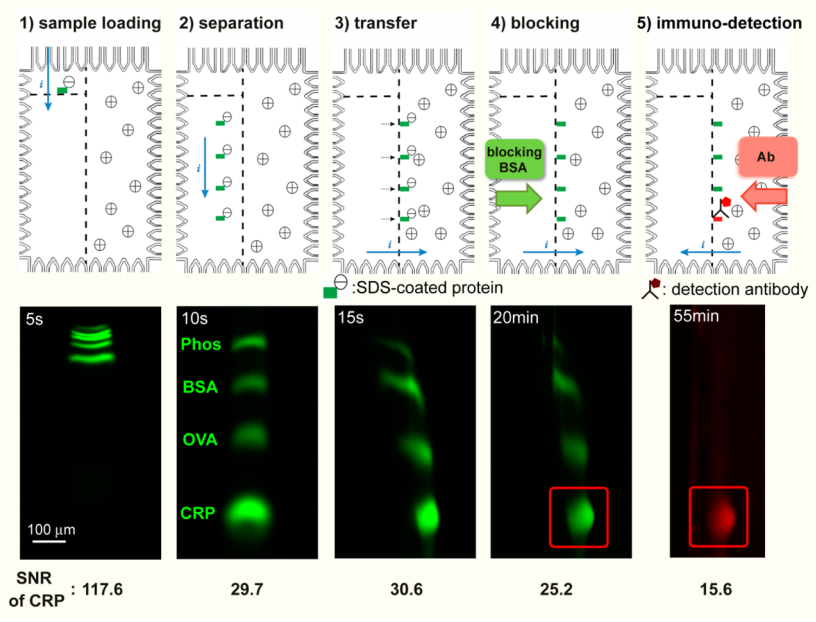


**Figure 4.** Multiple WB assay steps are integrated in the microchamber: step 1, protein sample plug injection; step 2, SDS-PAGE protein separation and sizing; step 3, electrotransfer and nonspecific blotting of separated proteins in the PL-PA blotting gel; step 4, blocking of nonspecific antibody binding sites on the PL-PA blotting gel; step 5, injection of antibody probe and readout of immunoblot. SNR change of CRP throughout the assay process is shown at the bottom.


dx.doi.org/10.1021/ac401012j | Anal. Chem. 2013, 85, 7753–7761

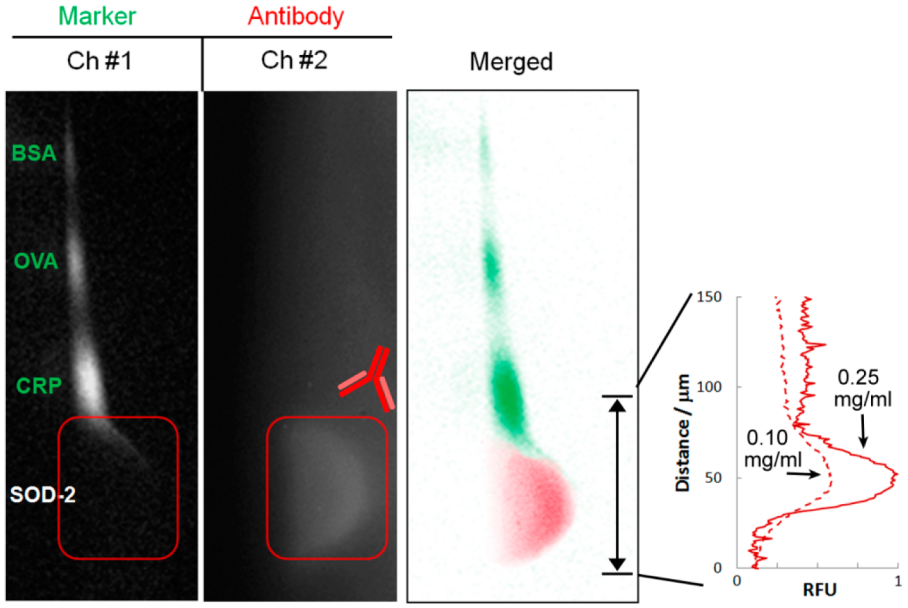


**Figure 5.** Multispectral imaging reveals specific immunoprobing of SOD-2 (unlabeled) in cell lysate. Spectral channel 1 reports green fluorescence, and spectral channel 2 reports red fluorescence signal. The merged image shows both the separation and probing results. Probing results for two different concentrations of SOD-2 in cell lysate are included in the right inset.

generally accepted as 80−100 nm,[29,30] the large PL may be proximal to electromigrating SDS−protein complexes and capture them like a "fishing rod".

The observation that proteins (including positively charged lactoferrin) remain bound to PL, even after some SDS removal, further suggests that other interactions may gain importance after the initial SDS−protein immobilization. It is plausible that the negatively charged proteins are more likely to be immobilized than positively charged proteins after SDS removal. To test the effect of native protein charge on immobilization, we compared the capture of high and low p*I* proteins with similar MW, lactoferrin (78 kDa, p*I* 8.7) and BSA (67 kDa, p*I* 4.7). The same amount of separated lactoferrin and BSA by SDS-PAGE were captured on the PL-PA blotting gel, and retention was simultaneously monitored (Figure S3 in the Supporting Information). Though the lactoferrin showed slightly lower capture possibly due to its positive charge, immobilization of both proteins was comparable, 65−70% for lactoferrin and 85−90% for BSA, respectively, regardless of their p*I*, attributed here to hydrophobic interaction with bound PL. Given an accepted SDS-to-protein ratio of 1.4 g of SDS per 1 g of protein[16] (i.e., 121 SDS molecules on a 25 kDa protein with a native charge not exceeding −10), the loss of up to −121 charge units owing to SDS dissociation would be significant. Once the protein and PL interact and result in protein immobilization, short-range interactions including hydrophobic interaction[31] and induced dipole particularly with highly charged PL may also become important after SDS dilution.[32,33]

**Antibody Probing of PL-Immobilized Protein.** After establishing the protein immobilization strategy, we introduced Ab based probing of immobilized target antigens (Ag). Inclusion of a blocking step and the probing step is required to complete the Western blot assay workflow (Figure 4). A protein ladder (500 nM each of AF488 labeled CRP, OVA, BSA, and Phos) was used for characterization.

After separation by SDS-PAGE and electrotransfer to a PL-PA blotting gel, a lateral electric field ($E$ = 45 V/cm) was applied to drive free SDS out of the PL-PA blotting gel and introduce blocking BSA (1 mg/mL of unlabeled BSA, 1× TG buffer) from reservoir no. 6. Electrostatic immobilization starting from the interface of the PL-PA blotting gel resulted in compression and enrichment as well as slight variation of peak position. As PL100 causes more peak compression, the variation [(peak shift)/(peak width) × 100)] of the peak is larger for PL100 (15%, $n$ = 4) than PL50 (5%, $n$ = 10), and the SR changes more for PL100 (from 2.2 to 1.5 for the least resolved BSA-OVA peaks) than PL50 (from 2.4 to 2.1 for BSA-OVA). High MW proteins such as Phos are more peak shifted because they are more compressed due to their low mobility. Use of an internal MW standard allows data comparison before and after immobilization.

A 15 min injection of blocking BSA was followed by a 5 min incubation period, during which fluorescently labeled detection antibodies were added to reservoir no. 7 to probe immobilized proteins. The polarity of the applied electric field was then reversed for 15 min so that Ab introduction and flushing of unbound blocking BSA out of the microchamber occurred simultaneously. Up to a 15% reduction (more loss for smaller proteins) of immobilized protein was observed during the blocking step (Figure 3). This loss results in diminished SNR (from 30.6 to 25.2 for CRP). For comparison, material losses observed during electrotransfer to nitrocellulose membranes in conventional slab-gel Western blotting is estimated to range from 89 to 29% for 30−98 kDa proteins.[34] Antibodies were conjugated with a positively charged red fluorophore (Atto 550, +1 charged) instead of negatively charged dye to reduce electrostatic binding to the positively charged PL. The Ab−Atto550 conjugate was negatively charged in the 1× TG buffer and electrophoretically introduced to the PL-PA blotting gel from reservoir no. 7. Ab was introduced from reservoir no. 7 to minimize accumulation of the Ab at the separation−blotting gel interface where the pore size is reduced abruptly. While pore-size discontinuities were minimized during development of the photopatterning process,[35] slight differences in the pore-size between the gel regions are observed. After a 15 min introduction and 5 min incubation, unbound Ab was


dx.doi.org/10.1021/ac401012j | *Anal. Chem.* 2013, 85, 7753−7761

electrophoresed out from the microchamber for ~10 min. Step 5 of Figure 4 shows probing results for anti-CRP Ab bound to immobilized CRP. The red Ab signal overlaps with the CRP band (SNR = 25.2) with an acceptable background (SNR = 15.6), suggesting specific interactions with the immobilized protein target. Quantitative antibody signal readout over a linear dynamic range of 3 logs was observed for CRP (Figure S4 in the Supporting Information).

**Microfluidic WB of SOD-2 in Whole Cell Lysate.** The complete SDS-PAGE microchamber Western blot was applied to analysis of superoxide dismutase 2 (SOD-2, 23 kDa) in cell lysate where Western blot is commonly used for protein measurement. SOD-2 was measured in a transfected 293T cell line derived from a human embryonic kidney. SOD-2, which exists as a homotetramer with 23 kDa individual subunits, is a mitochondrial antioxidant enzyme for protecting against oxidative damage.[36] The SOD-2 is a good example to demonstrate how the PL-PA gel can be optimized because of its high electrophoretic mobility.

We analyzed unlabeled SOD-2 containing lysate mixed with a protein ladder (50 nM each of AF488 labeled CRP, OVA, and BSA), as shown in Figure 5. To enhance the analytical sensitivity of the assay, we performed an iterative injection-separation-immobilization process on the sample to raise the total amount of SOD-2 mass immobilized on the PL-PA blotting gel. The multiple injections were necessary, as the immobilization efficiency of SOD-2 was observed to be low owing to high electrophoretic mobility and low starting SOD-2 concentration; protein concentration of the lysate was 0.5 mg/mL and further diluted by half with addition of the protein ladder. An increased concentration (2.4 $\mu$M) of PL100 was incorporated to the PL-PA blotting gel to further enhance protein capture. Owing to the higher charge than previously used, the blocking step was performed with a 2× longer incubation duration than in the PL100 PL-PA blotting gel. Figure 5 shows the results of the SOD-2 assay. The ladder is clearly visible in the green spectral channel, with no detectable (unlabeled) SOD-2. Imaging the red spectral channel reports that the location of antibody against SOD-2 (23 kDa) is slightly below CRP (25 kDa), around the anticipated molecular mass location considering the log−linear MW vs mobility relation. The quantitative comparison for different lysate concentrations (0.25 mg/mL and 0.10 mg/mL) shows a concomitant response of probing antibody signal (Figure 5 inset). The SOD-2 result demonstrates the capacity of the microchamber assay to report molecular mass and immunoaffinity for an unlabeled target protein even amidst a complex proteinaceous background (lysate).

## CONCLUSION

Our work details the development, optimization, and characterization of an integrated microfluidic Western blot capable of pan-analyte immobilization of SDS-coated protein after SDS-PAGE for antibody probing. The functionally patterned microchamber has proven to be a well-suited format for single-chip integration of multistep analysis and substantially advanced microfluidic integration of Western blotting with automated fluidic manipulation. Our work significantly extends the applicability of the microchamber to the most commonly used protein sizing technique, SDS-PAGE. The rapid, quantitative capabilities of the device is demonstrated in both purified proteins and unlabeled protein in crude cell lysate with enhanced performance of 100× reduction of sample consumption, 10× reduction in assay duration, and automated assay operation, compared to conventional slab-gel Western blotting. Systematic study of the immobilization mechanism is presented by controlling PL characteristics and by monitoring the folding state of immobilized proteins. The accessibility between PL and migrating protein influences the immobilization efficiency and binding rate. Electrostatic attraction is responsible for the initial binding of SDS-coated protein to the PL. However, once the proteins are bound, hydrophobic interaction seems to be important to maintain binding after SDS removal.

The microchamber immunoblotting assay design may be adaptable to analyses of multiple specimens, including when comparison of two samples is needed (i.e., healthy control and specimen of interest). Possible design approaches to support multiplexing include introducing a microchamber with a central separation region flanked on either side by a blotting region (two blotting regions total). As no sample is immobilized in the separation channel, reuse of the separation channel is feasible and the two blotting regions would allow same-chamber comparison of readout. We could also envision using multiple fluorophores to label the sample, as well as probe readout, allowing concurrent analysis of multiple biospecimens where simultaneous probing of multiple targets is feasible[7] (i.e., akin to a difference gel electrophoresis (DIGE) analysis but with immunoprobing). Lastly, as the size of microchamber occupies a small portion of the entire chip surface area, we could envision multiple chambers housed on a single glass chip to support analyses of multiple samples on one device.

While no one assay or device is relevant to all measurement needs, the system detailed offers advantages in specific aspects of both usage mode and performance, as compared to (for example) commercially available capillary based immunoprobing systems. With respect to usage and adoption, the present system requires no external actuation beyond application of electrical potentials (i.e., no additional pumping, valving, or UV light exposure hardware). Further, the present system is compatible for readout using existing laboratory infrastructure, such as microarray scanners. With respect to performance, blotting efficiency can be readily optimized by adjusting both transport and materials properties. This may be important in mitigating blotting bias that can occur owing to differences in physicochemical properties of target proteins in a single sample. For example, the PL-PA gel could be spatially varied to allow for higher charge densities in blotting regions with high mobility species. Finally, owing to use of a volume-based blotting approach[10] (i.e., capture on a channel-filling hydrogel, as opposed to a functionalized capillary surface), the current assays achieves near-complete protein capture in reduced run times, as compared to existing capillary technologies.

Coupled with detailed characterization of the immobilization mechanism, microfluidic integration of SDS-PAGE with blotting and probing may rival the conventional Western blot in general biology and clinical laboratories.

## ASSOCIATED CONTENT

### Supporting Information

Device fabrication procedures, figures for biotinylation of PL and relative fluorescence intensity change by SDS concentration, and a table with the assay operation program. This material is available free of charge via the Internet at http://pubs.acs.org.

## AUTHOR INFORMATION


### Corresponding Author

*E-mail: aeh@berkeley.edu.

### Present Address

[§]D.K.: Department of Mechanical Engineering, Myongji University, Yongin, Gyeonggi-do 449-728, South Korea.


### Notes

The authors declare no competing financial interest.

## ACKNOWLEDGMENTS

The authors gratefully acknowledge the Graham R. Fleming group (Chemistry at UC Berkeley) for allowing us to use a fluorimeter. This work was supported by the University of California (UC) Discovery Grant and the Industry-University Cooperative Research Program (IUCRP). A.E.H. is an Alfred P. Sloan Foundation Research Fellow in Chemistry.

## REFERENCES


(1) Laemmli, U. K. *Nature* **1970**, *227*, 680−685.
(2) Towbin, H.; Staehelin, T.; Gordon, J. *Proc. Natl. Acad. Sci. U.S.A.* **1979**, *76*, 4350−4354.
(3) Hu, S.; Xie, Z.; Qian, J.; Blackshaw, S.; Zhu, H. *Wiley Interdiscip. Rev. Syst. Biol. Med.* **2011**, *3*, 255−268.
(4) He, M.; Herr, A. E. *Nat. Protoc.* **2010**, *5*, 1844−1856.
(5) He, M.; Novak, J.; Julian, B. A.; Herr, A. E. *J. Am. Chem. Soc.* **2011**, *133*, 19610−19613.
(6) Hou, C.; Herr, A. E. *Analyst* **2012**, *138*, 158−163.
(7) Tia, S. Q.; He, M.; Kim, D.; Herr, A. E. *Anal. Chem.* **2011**, *83*, 3581−3588.
(8) Kim, D.; Karns, K.; Tia, S. Q.; He, M.; Herr, A. E. *Anal. Chem.* **2012**, *84*, 2533−2540.
(9) Hughes, A. J.; Lin, R. K.; Peehl, D. M.; Herr, A. E. *Proc. Natl. Acad. Sci. U.S.A.* **2012**, *109*, 5972−5977.
(10) Hughes, A. J.; Herr, A. E. *Proc. Natl. Acad. Sci. U.S.A.* **2012**, *109*, 21450−21455.
(11) Starita-Geribaldi, M.; Sudaka, P. *Bioseparation* **1990**, *1*, 111−117.
(12) Dunn, S. D. *Anal. Biochem.* **1986**, *157*, 144−153.
(13) De, S.; Girigoswami, A.; Das, S. *J. Colloid Interface Sci.* **2005**, *285*, 562−573.
(14) Hazra, P.; Chakrabarty, D.; Chakraborty, A.; Sarkar, N. *Biochem. Biophys. Res. Commun.* **2004**, *314*, 543−549.
(15) Gelamo, E. L.; Silva, C. H.; Imasato, H.; Tabak, M. *Biochim. Biophys. Acta* **2002**, *1594*, 84−99.
(16) Reynolds, J. A.; Tanford, C. *Proc. Natl. Acad. Sci. U.S.A.* **1970**, *66*, 1002−1007.
(17) Hogset, A.; Prasmickaite, L.; Tjelle, T. E.; Berg, K. *Hum. Gene Ther.* **2000**, *11*, 869−880.
(18) Needham, L.; Hellewell, P. G.; Williams, T. J.; Gordon, J. L. *Lab. Invest.* **1988**, *59*, 538−548.
(19) Liu, G.; Molas, M.; Grossmann, G. A.; Pasumarthy, M.; Perales, J. C.; Cooper, M. J.; Hanson, R. W. *J. Biol. Chem.* **2001**, *276*, 34379−34387.
(20) Sadana, A.; Vo-Dinh, T. *Appl. Biochem. Biotechnol.* **1997**, *67*, 1−22.
(21) Bharadwaj, R.; Park, C. C.; Kazakova, I.; Xu, H.; Paschkewitz, J. S. *Anal. Chem.* **2008**, *80*, 129−134.
(22) Squires, T. M.; Messinger, R. J.; Manalis, S. R. *Nat. Biotechnol.* **2008**, *26*, 417−426.
(23) Luchowski, R.; Matveeva, E. G.; Gryczynski, I.; Terpetschnig, E. A.; Patsenker, L.; Laczko, G.; Borejdo, J.; Gryczynski, Z. *Curr. Pharm. Biotechnol.* **2008**, *9*, 411−420.
(24) Zhuang, X.; Ha, T.; Kim, H. D.; Centner, T.; Labeit, S.; Chu, S. *Proc. Natl. Acad. Sci. U.S.A.* **2000**, *97*, 14241−14244.
(25) Israelachvili, J. N. *Intermolecular and Surface Forces*; Academic Press: New York, 1985.
(26) Yasui, S. C.; Keiderling, T. A. *J. Am. Chem. Soc.* **1986**, *108*, 5576−5581.
(27) Aharoni, S. M.; Crosby, C. R.; Walsh, E. K. *Macromolecules* **1982**, *15*, 1093−1098.
(28) Kikuchi, K.; Yoshioka, K. *Biopolymers* **1973**, *12*, 2667−2679.
(29) Holmes, D. L.; Stellwagen, N. C. *Electrophoresis* **1991**, *12*, 253−263.
(30) Stellwagen, N. C. *Electrophoresis* **2009**, *30* (Suppl 1), S188−195.
(31) Chen, W.-Y.; Huang, H.-M.; Lin, C.-C.; Lin, F.-Y.; Chan, Y.-C. *Langmuir* **2003**, *19*, 9395−9403.
(32) Schreiber, G.; Fersht, A. R. *Nat. Struct. Biol.* **1996**, *3*, 427−431.
(33) Zhou, H. X. *Biopolymers* **2001**, *59*, 427−433.
(34) Bolt, M. W.; Mahoney, P. A. *Anal. Biochem.* **1997**, *247*, 185−192.
(35) Hou, C.; Herr, A. E. *Anal. Chem.* **2010**, *82*, 3343−3351.
(36) Zelko, I. N.; Mariani, T. J.; Folz, R. J. *Free Radical Biol. Med.* **2002**, *33*, 337−349.